

Article

Research on the Soil-Plugging Effect on Small-Diameter Jacked Piles through In Situ Testing and DEM Simulation

Xueyan Wang ¹, Yuan Mei ^{2,3}, Yili Yuan ^{2,*}, Rong Wang ⁴ and Dongbo Zhou ²¹ School of Urban Planning and Municipal Engineering, Xi'an Polytechnic University, Xi'an 710048, China² School of Civil Engineering, Xi'an University of Architecture & Technology, Xi'an 710055, China³ Shaanxi Key Lab of Geotechnical and Underground Space Engineering, Xi'an 710055, China⁴ Xi'an Traffic Engineering Institute, Xi'an 710300, China

* Correspondence: yiliyuan@xauat.edu.cn; Tel.: +86-13087540698

Abstract: Small-diameter jacked piles are widely used in civil engineering. The formation and development of the soil-plugging effect and surface frictional behavior of jacked piles have a high impact on the construction process and pile quality. Clarifying the developmental pattern of the soil-plugging effect and the change law of frictional force forms the premise of scientific construction and construction quality. Firstly, we carried out two groups of in situ tests on the small-diameter jacked piles, recording the relationship between penetration depth and resistance force. Then, the discrete element method (DEM) was used to analyze the mechanical behavior of the small-diameter jacked piles during the construction process. The particle flow code (PFC) 2D was used to carry out the DEM simulation. The research results show that pile resistance exhibited an irregular development trend as the construction process proceeded. There is a sudden change in pile resistance when the pile tip reaches the interface of certain soil layers. Both tests revealed the same phenomenon, yet both occurred at different depths. The DEM analysis showed that plug sliding was the main reason for the above phenomenon. The difference in strength and stiffness of adjacent soil layers causes the soil plug to slide, leading to a sudden change in pile resistance. When the upper layer is soft and the layer below is hard, this phenomenon is especially obvious. This also leads to a difference in the location of the sudden change in pile resistance between the two groups of tests. The research results of this paper can be helpful for revealing the relationship between the soil-plugging effect of small-diameter jacked piles and the development of pile resistance and also provides a reference for relevant engineering construction and design.

Keywords: small diameter jacked pile; in situ testing; soil-plugging effect; discrete element method

Citation: Wang, X.; Mei, Y.; Yuan, Y.; Wang, R.; Zhou, D. Research on the Soil-Plugging Effect on Small-Diameter Jacked Piles through In Situ Testing and DEM Simulation. *Buildings* **2022**, *12*, 2022. <https://doi.org/10.3390/buildings12112022>

Academic Editors: Bingxiang Yuan, Yong Liu, Xudong Zhang, Yonghong Wang and Jiho Moon

Received: 26 August 2022

Accepted: 14 November 2022

Published: 18 November 2022

Publisher's Note: MDPI stays neutral with regard to jurisdictional claims in published maps and institutional affiliations.



Copyright: © 2022 by the authors. Licensee MDPI, Basel, Switzerland. This article is an open access article distributed under the terms and conditions of the Creative Commons Attribution (CC BY) license (<https://creativecommons.org/licenses/by/4.0/>).

1. Introduction

Small-diameter jacked piles are widely used in urban foundation engineering because of their high bearing capacity, low cost, and low construction noise. Strengthening the uneven settlement of the existing building foundation through the use of jacked piles can not only raise the reinforcement quality of the foundation but also ensure building safety and environmental protection [1]. It can be applied to various soils and has become the most preferred scheme of foundation treatment. In order to understand its construction properties, researchers have used model tests, in situ tests, and numerical analysis to study the penetration characteristics and pile resistance of jacked piles.

In terms of tests, Lehane and Gavin [2] studied the relationship between the foundation stiffness and the bearing capacity of soil plugs through indoor model tests. Vesic [3] analyzed the change in pile tip resistance and proposed the critical depth of the pile according to the results of the field tests. Randolph et al. [4] studied the influence of foundation consolidation history on pile stress through parameterization analysis. In the process of pile penetration via jacked piles, the soil-squeezing effect and soil-plugging effect coexist.

The existence of the soil plug has a great influence on the characteristics of pile penetration and the development of the bearing capacity, which makes the engineering characteristics of jacked piles very different from other kinds. Murthy et al. [5] studied the formation characteristics of soil plugs during pile construction using laboratory model tests. They also obtained the influence of pile diameter, pile pressure, and penetration depth on soil plugs based on data analysis. Hailei et al. [6] conducted experimental fluctuant research on the mechanical performance of model piles under different penetration rates and obtained the relationship between the pile penetration rates and the size of the soil plug. Based on the cavity expansion theory, Li et al. [7] proposed a calculation formula for pile resistance considering the influence range of pile tip resistance during the penetration process in soft soil layers. Lehane and Gill [8] and Cao et al. [9] obtained the displacement field of the soil around jacked piles and the deformation law inside the soil during pile penetration based on transparent soil material; the result is interesting, but transparent soil is still separate from natural sand, which should be further studied. Liu et al. [10] and Sang et al. [11] used the micro FBG-MEMS pressure-sensing technique to monitor the stress of the pile during the penetration process. They concluded that the pile resistance force (when constructing in a homogeneous soil layer) also increased in waves, and side resistance degenerated at the same depth. Kodsy and Iskander [12] analyzed the soil plug effect of 74 groups of jacked tubular piles with different sizes. With the help of fiber Bragg grating sensor technology, Kou et al. [13] analyzed the interaction feature of the frictional force between the inner wall and outer wall of the jacked tubular pile influenced by the soil plug. Han et al. [14] conducted field tests using both static and dynamic loads on jacked piles. They also compared the resistance force measured by static load tests with the resistance force obtained by static cone penetration tests.

On the other hand, various numerical simulation methods were established and used in the analysis of jacked piles, such as the conventional finite element method [15,16], arbitrary Lagrangian-Eulerian (ALE) method [17–20], coupled Eulerian-Lagrangian (CEL) method [21], material point method (MPM) method [22–24], smooth particle hydrodynamics (SPH) method [25,26], and the discrete element method (DEM) [27,28]. Hong and Xueyi [29] used FEM simulation to analyze the soil-squeezing effect of static pressure piles based on spherical cavity expansion theory. Lorenzo et al. [23] used the material point method to simulate the penetration process of jacked piles, proving the feasibility of the material point method. Ko et al. [21] simulated the driving process of open-ended piles in sand using the coupled Eulerian-Lagrangian (CEL) approach; the parametric analysis revealed that the plugging effect was mostly influenced by driving energy, followed by pile diameter and pile embedment depth. Hu et al. [30] used the Voigt model to treat the soil plug as an additional mass attached to the pile body and considered the compactness of the soil plug in their study. Their research shows that the thickness of the pile influences the expansion pressure as well as the dynamic effect of the soil plug on the pile. Liu et al. [31] established a discrete element model of the penetration response of jacked piles considering different diameters, which qualitatively reflects the changing trends in soil flow, soil plugging, pile resistance, and the stress distribution of the soil, but it is hard to directly use in practice. Among all numerical methods, DEM is particularly suitable for the mechanism analysis of soil materials because it provides a convenient and comprehensive alternative to investigate both the macroscopic and microscopic behavior of granular soil [28,32].

Most of the above studies focus on homogeneous soil layers. Few studies involve in situ testing or analyzing the formation and development mechanism of the penetration process, plugging effect, soil-arching effect, and other characteristics in detail. In this paper, the penetration process of a small-diameter jacked pile is analyzed through a set of in situ tests in the soft foundation of a garbage backfill engineering site. The discrete element method was used to simulate the penetration process of the in situ testing. The pattern of change for soil plug thickness and pile resistance are analyzed based on the in situ testing data and the result of the DEM simulation. The research results of this paper are expected

to provide a reference for similar projects and provide a theoretical basis for the design and construction of small-diameter jacked piles.

2. In Situ Tests of Small-Diameter Jacked Pile

2.1. Engineering Background of the In Situ Test

The in situ testing in this paper was conducted during a strengthening engineering project in Xi'an, Shaanxi Province. The soil foundation consisted of 5 layers: the ① artificial plain filling layer, ② filling sand layer, ③ medium sand layer, ④ silty clay layer, and the ⑤ coarse sand layer. The thicknesses and engineering properties of the layers vary strongly, and their positional relationship is not fixed. For instance, the minimum fill thickness of the artificial fill layer is 1.8 m, while the maximum value is 4.3 m. The distribution and engineering properties of each soil layer are shown in Table 1. The widely distributed artificial plain filling layer is an uncompacted, irregular, and uneven deposit body, which is backfilled after soil borrowing. The soil quality of the artificial plain filling layer is relatively loose and has high porosity, which can be classified as under-consolidated soil. Under-consolidated soil is compacted by its own weight, and precipitation infiltration has an influence on the situation during the construction and service period, resulting in a large area of uneven settlement surrounding nearby buildings. The maximum settlement had already been reached at 180 mm during this engineering project. Therefore, reinforcements were needed to control the settlement.

Table 1. Soil layer distribution and engineering properties.

Label	Layer Name	Thickness (m)	Bearing Capacity (kPa)	Bulk Density/ γ (KN/m ³)	Cohesive/c (kPa)	Angle of Friction/ ϕ (°)	Modulus of Compressibility/ E_s (MPa)
①	Artificial plain filling	0.5~3.9	85	15.2	10	10	4.8
②	Filling sand	0.3~2.4	150	17.6	5	18	12.5
③	Medium sand	0.7~5.4	200	19	/	28	20.3
④	Silty clay	0~0.5	160	17.9	30	22	5.1
⑤	Coarse sand	1.1~3.9	250	19.5	/	30	25.7

2.2. Test Principle and Purpose

Through the in situ penetration tests carried out in the soft foundation of the site, the pile penetration mechanism of the small-diameter jacked piles under static pressure was studied. The variation law of the resistance force of the pile during the penetration process, along with the penetration depth under different soil conditions, was analyzed. The construction performance of small-diameter jacked piles in strengthening engineering was also explored.

Before the penetration process of the test, four anchor bolts were embedded around the pile in advance, serving as a reaction frame. Hydraulic jacks were used to gradually press the pile into the soil. After pile penetration was completed, concrete was poured to seal the pile. The pile penetration speed was kept constant during the test process and the pile penetration process was considered a uniform linear motion. For buildings that have already settled, the essence of strengthening engineering is to transform the independent foundation form into a composite foundation, in which piles and soil work together [33,34]. Part of the load of the building will be transferred to the soil through the jacked piles so as to reduce the pressure of the independent foundation on the foundation soil to limit the settlement of the foundation and achieve the purpose of reinforcement [35].

The penetration process of a small-diameter jacked pile is more stable than other types, such as those that are hydraulic hammer-based. The applied static hydraulic force must overcome the friction force around the side surface of the pile and the tip resistance force

generated in the penetration process, which is affected by the engineering properties of the soil layer, pile length, depth of penetration, and so on. In general, jacked piles cause complex movements and force onto the soil during penetration (and vice versa). When the pile penetrates, the soil below the pile tip will be compressed and produces excess pore water pressure [36]. When the penetration pressure increases, the pile tip will break into the soil, causing the soil to undergo the accompanying direct shear failure. The soil inside and outside the pile move simultaneously in the beginning. The soil exerts both friction force and normal force on the pile surface at this stage. When the soil plug emerges, the soil inside the pile will stay still in the front and cause tip pressure to the pile. Plug length may also change during the penetration process because of the soil movement. The total resistance force of the pile may change randomly depending on the state of the soil plug. Therefore, to study the soil-plugging effect on small-diameter jacked piles, the total resistance force of the pile was monitored.

2.3. Test Steps

As shown in Figure 1, a small-diameter steel pipe pile with a diameter of 180 mm and a wall thickness of 8 mm was chosen. Other test devices include a hydraulic jack, a high-pressure oil pump, and a reaction frame. Before the test, four M24 antifloat anchors were buried around the pile hole, and the reaction frame was assembled accordingly. Then steel pipe pile was positioned, and its verticality was checked. The length of each standard section of the piles is 2 m. During penetration, the pressure value of the oil pump was recorded every 0.2 m. The pile penetration speed was kept at 0.4 m/min. As shown in Figures 2 and 3, two locations with distinguished strata were chosen for running the test. Six test piles, three for each location, were independently constructed.

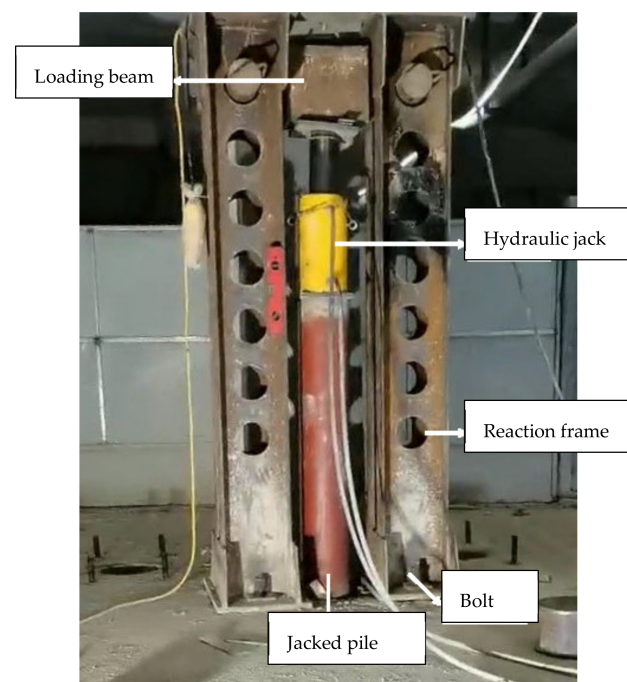


Figure 1. In situ test of small-diameter jacked pile.

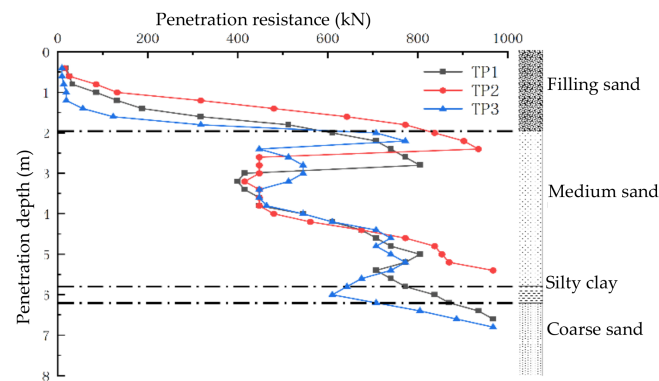


Figure 2. Penetration resistance curve for condition *a*.

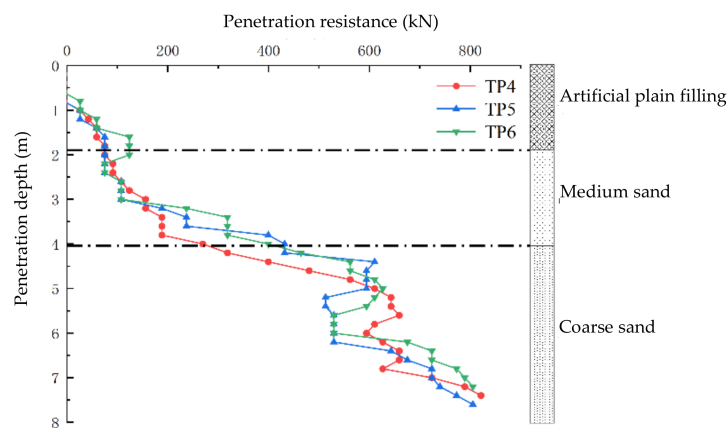


Figure 3. Penetration resistance curve for condition *b*.

3. Processing and Analysis of the In Situ Test

Since the penetration speed was kept to a low value, the penetration process can be seen as quasistatic. Therefore, the total pile resistance force can be obtained as the force calculated from the oil pump. Figures 2 and 3 show the variation curves of the penetration resistance of the pile, with the penetration depth of the two conditions. In the figures, TP stands for test pile. There are 6 test piles in total. It can be seen that, under the same soil distribution, the variation trend of the test piles is basically the same, indicating that the variation in pile penetration resistance has a certain regularity.

For condition *a*, it can be seen from Figure 2 that the change law of pile penetration resistance of the small-diameter jacked pile is highly related to the soil layers. When the test piles entered the filling sand layer, due to the large shaking of the test pile, the growth rate of penetration resistance was low. Then, the pile penetration resistance increased rapidly when the penetration depth was nearly 0.5 m, denoting that the soil plug began to form. When the pile tips started to enter the medium sand layer, the penetration resistance force peaked at 805 kN, 935 kN, and 772 kN, respectively, for the three test piles. In the upper part of the medium sand layer, the penetration resistance decreased by about 50%. In the thicker medium sand layer, due to the nonuniformity of the soil, the pile penetration resistance also changed slightly, but it still showed an increasing trend. When the pile tip enters the silty clay layer, the pile penetration resistance encounters a second inflection point. It can be seen that, within complex geological conditions, the hardness of the soil has a direct impact on pile penetration resistance [37].

For condition *b*, the changing trend of the three test piles in Figure 3 is quite different from that in Figure 2. Because the artificial plain fill layer is relatively soft and the external disturbance is large, the pile penetration resistance in this layer is small. At the junction of the artificial plain fill and the medium sand layer, the pile penetration resistance was only 74 kN, 82 kN, and 123 kN for the three test piles. When the pile tips entered the medium

sand layer, the growth rate of the pile penetration resistance increases, but the change is moderate compared to condition *a*, as shown in Figure 2. This is mainly caused by the interaction between adjacent layers and the small compaction degree of the medium sand layer in this area. As the penetration proceeds, there is an inflection point in the penetration resistance curve when the pile tip enters the upper part of the coarse sand layer. The mutation is small: 7.4%, 13.7%, and 10.9%, respectively. Penetration resistance continues to increase in the middle and lower part of the coarse sand layer. The changing trend is not obvious; the values reached 821 kN, 805 kN, and 801 kN, respectively.

The phenomenon of the sudden increase or decrease in the growth rate of penetration resistance occurs during pile penetration and is mainly related to the geotechnical nature of the soil layer at the tip and side of the pile, the penetration depth, and other factors. The above analysis is only a qualitative analysis of the obtained pile penetration resistance data based on limited stratum data and construction experience, which cannot quantitatively describe the change mechanism for pile penetration resistance, the soil plug effect, and the soil-arching effect during the penetration process. The following part of this paper will analyze the in situ test processes with the help of the discrete element method (DEM) to study the change in pile penetration resistance and reveal the mechanism between penetration resistance and the soil plugging effect.

4. Discrete Element Numerical Simulation Analysis of the Small-Diameter Jacked Pile

4.1. DEM Modeling of the Small-Diameter Jacked Pile

4.1.1. Geometric Model

In the present study, considering the calculation cost of practical usage, PFC2D was used to model the pile penetration process of the in situ tests. The discrete element model of the in situ test process of the small-diameter jacked piles includes three parts: test piles, soil containers, and soil layers. The stiffness of the piles and soil is relatively large [38,39], and the deformation of the steel pipe pile has little effect on the simulation results; therefore, the steel pipe pile was considered to be a rigid wall. Since the model is two-dimensional, the test piles are simplified into two parts: the left wall and the right wall. The soil container is composed of three rigid walls. In order to avoid the boundary effect and also decrease the calculation costs, the container size was set to 2.8 m (15 times that of the pile diameter) in the horizontal direction and 10 m in the longitudinal direction (Figure 4). The soil particles were modeled with two-dimensional discs. Considering the gradation curve and void ratio of each soil layer, the proportional method and expanded radius method were used to gradually generate the soil particles. The total number of particles is 35,000. The constitution model and the contact parameters of the soil particles were assigned according to the stratum information in Figures 2 and 3 and Table 1. Two discrete element models were obtained according to the two test conditions. It should be mentioned that, strictly speaking, the 2D model follows the plane strain assumption, and therefore the modeled piles should be considered empty wall structures rather than piles. However, the purpose of this study is to explain the mechanism of the soil plugging effect on the small-diameter jacked pile during the construction process and to qualitatively analyze the relationship between the plug length and penetration resistance. Additionally, the use of 2D DEM for pile penetration has already been verified by many researchers [40–44]. Therefore, a 2D DEM model was used.

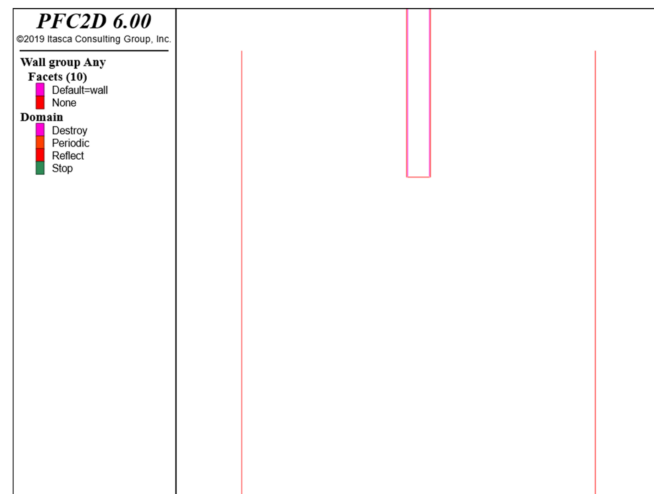


Figure 4. Soil container and pile model from the DEM model.

4.1.2. Calibration of Contact Parameters

In this paper, the trial-and-error method was used to calibrate the parameters of the contact parameters of each layer of soil. Among them, the linear-bonding model was used for layers ①, ②, and ④, and the linear model was used for layers ③ and ⑤. In order to carry out the trial-and-error method, a numerical triaxial test was established using the same particle settings of the in situ test simulation. Random contact parameters were then input to run the DEM simulation. The analysis results were compared with the actual performance of the material. The parameters were then manually adjusted according to the comparison results until the input parameters made the model analysis results meet our expectations. The contact parameters in the model include the friction coefficient, $fric$, the tensile and shear strength, cb_tens and cb_shears , the contact stiffness modulus, E_{mod} , and the normal tangential stiffness ratio, K_{ratio} . The calibration results are shown in Table 2.

Table 2. Calibration results.

Label	Layer Name	Fric	$cb_tens(cb_shears)$ 10^2 kPa	Kratio	$E_{mod}/$ 10^4 kPa
①	Artificial plain filling	0.57	2.18	2.62	2.42
②	Filling sand	0.91	1.52	3.08	8.21
③	Medium sand	1.32	/	1.71	15.34
④	Silty clay	1.56	10.69	3.53	3.72
⑤	Coarse sand	2.21	/	3.16	20.18

4.1.3. Determination Off-Loading Rate

The loading rate is one of the most important simulation parameters in the DEM. Figure 5 shows a comparison of the shear strength indexes and different loading rates. It can be seen that the loading rate has a significant impact on the cohesion of the soil but has a small impact on the internal friction angle. When the loading rate is less than 0.02 m/s, a lower loading rate will have little impact on the results. Therefore, considering the calculation cost and simulation accuracy, the loading rate was set to 0.02 m/s in this paper.

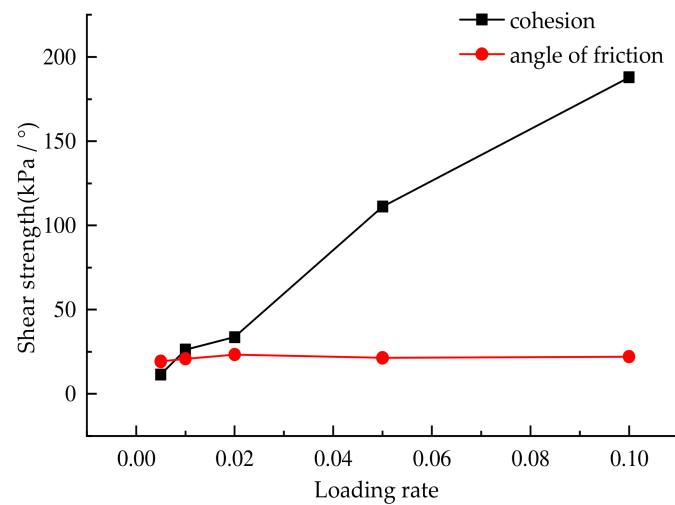


Figure 5. Influence of loading rate on shear strength.

4.2. Simulation Process and Results

In the simulation, the piles were statically pressed at a speed of 0.02 m/s, and the relationship between the vertical reaction force on the modeled walls that represent the test piles and the displacement was recorded to reflect the pile penetration resistance curve. The friction of the inner walls was extracted to analyze the stress characteristics. Moreover, the change in the length of the soil plug was also obtained to analyze the soil plug effect during the construction using the small diameter jacked piles. As shown in Figure 6 is the initial state of the model. Figures 7 and 8 show the simulation results for condition a and condition b, respectively.

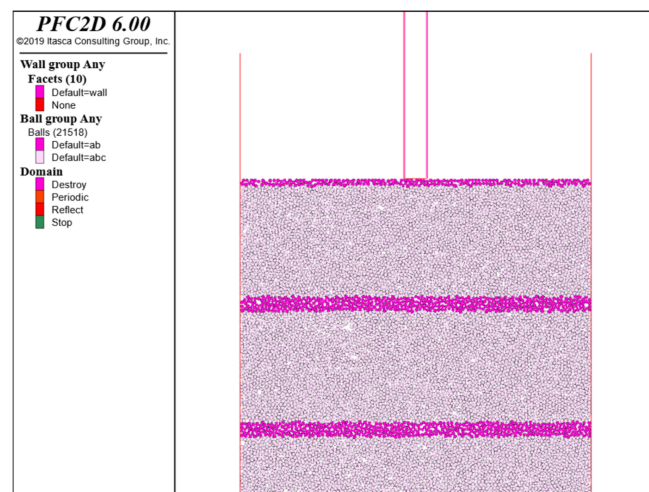


Figure 6. Modeling of soil particles.

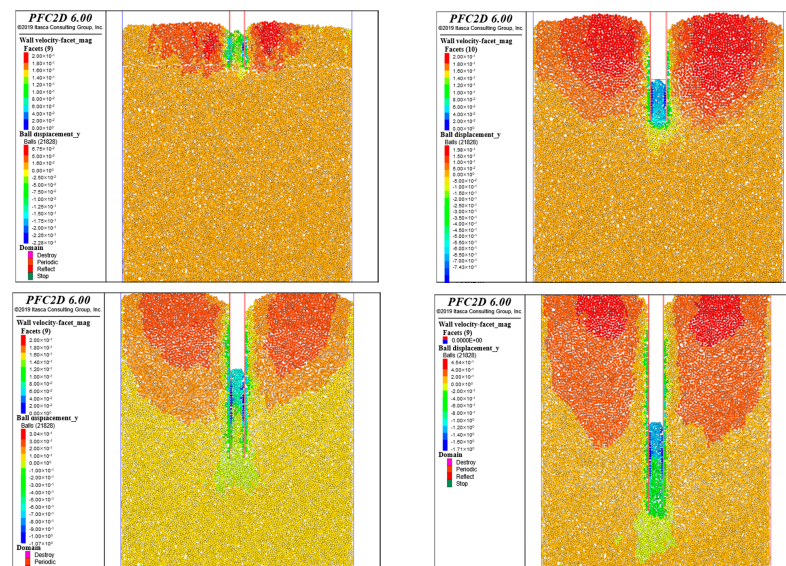


Figure 7. Simulation results of condition *a*.

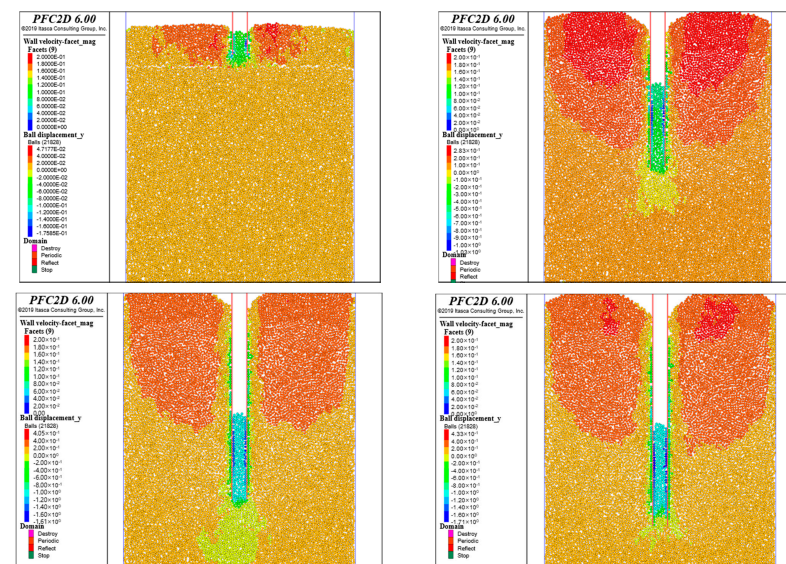


Figure 8. Simulation results of condition *b*.

4.3. Analysis of the Simulation Results

4.3.1. Soil Plug Length

The trend of soil plug length (the distance from the soil's surface in a pile to the pile bottom) variation with time was extracted, as shown in Figure 9 (condition *a*) and Figure 10 (condition *b*). For condition *a*, it is clear that the development curve for soil plug length with penetration depth can be divided into four stages: 0–1 m, 1–2 m, 2–4 m, and 4–6 m. The curve has a stagnation point when the pile penetration depth is around 1 m. Before that, the soil plug length increases approximately in a linear fashion. When the penetration depth is 1–2 m, the soil plug length almost remains unchanged. When the pile penetration depth is 2–4 m, there is a second approximate linear growth stage. Finally, in the last 4–6 m stage, there is another stable stage for the soil plug length. Compared with Figure 2, it can be seen that when the depth is about 1 m, the pile penetration resistance switches from a slow-growth mode to a fast-growth mode. This change is caused by the fact that, at 1 m, the lower soil particles in a pile are blocked by the upper soil plug particles, making the soil at the tip of the pile more and more dense, forming a soil arch and finally developing

the soil plug. As a result, the bottom soil plug in a pile begins to bear the soil pressure at the pile tip, so the pile penetration resistance increases rapidly.

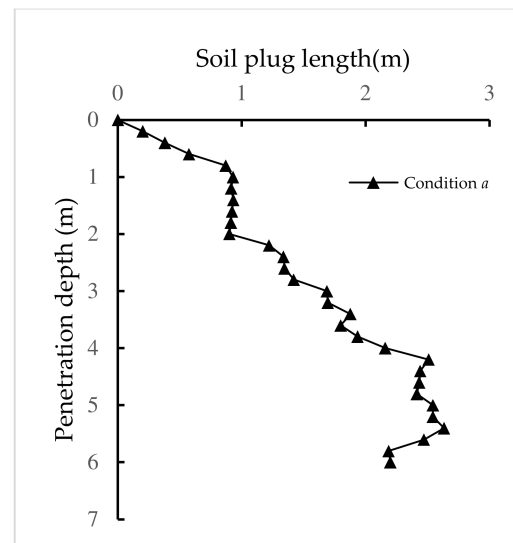


Figure 9. Soil plug length curve for condition *a*.

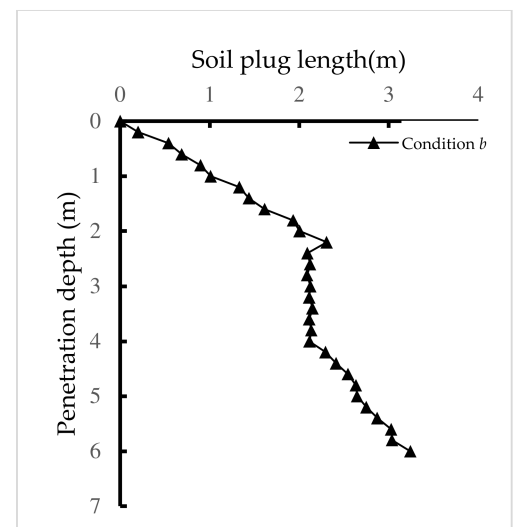


Figure 10. Soil plug length curve for condition *b*.

In Figure 9, the length of the soil plug began to increase when the penetration depth exceeded 2 m. This is because the pile tip entered the middle sand layer from the filling sand layer. As the compression modulus and strength of the middle sand layer are significantly higher than that of the filling sand layer, the soil arch temporarily failed. The friction status between the soil plug and the pile changed from static to dynamic, and the effect of the soil plug was ineffective at this moment. Therefore, the pile penetration resistance plummeted. During the 2–4 m stage, the length of the soil plug increased gradually, and the pile penetration resistance basically remained unchanged. After about 4 m, the soil plug formed again. It can be seen from Figures 2 and 9 that the length of the soil plug no longer increased, and the pile penetration resistance began to rise rapidly again at the same depth.

Similarly, Figures 3 and 10 show the relationship between penetration resistance and soil plug length for condition *b*. It can be seen that the development curve of soil plug length with penetration depth can be divided into three stages: 0–2 m, 2–4 m, and 4–6 m. The length of the soil plug increases linearly before the pile penetration depth reaches 2 m, which is in accordance with the slow linear increase stage of pile penetration resistance in

the early period in Figure 10. This is because the surface soil in test condition *b* is composed of the plain fill layer, the compression modulus and strength of which are too low to form a soil plug. When the pile tip enters the medium sand layer, the soil plug forms slowly. At this time, the length of the soil plug no longer changes within the 2–4 m stage, and the pile tip resistance of the soil plug begins to work, meaning the pile penetration resistance rises sharply.

Similar to condition *a*, when the pile penetration depth reached 4 m, the pile touched the coarse sand layer, and the strength and stiffness of the coarse sand layer were greater than that of the medium sand layer. For the same reason, the effect of soil arching on the soil plug temporarily fails, with the soil plug length then gradually increasing, while the pile penetration resistance remains almost unchanged.

4.3.2. Lateral Resistance

In order to further understand the composition and change mechanism of the penetration resistance of the test piles, the frictional resistance between the soil particles and both the inner and outer surface of the piles was obtained by calculating the resultant force in the Y-direction, as shown in Figures 11 and 12. It can be seen that the total friction is different in value from that in Figures 2 and 3, but the overall trend is consistent, and it can also correspond to the changing trend in soil plug thickness.

By comparing and analyzing the changing pattern of the inner and outer frictional resistance, we concluded that the outer frictional resistance basically maintains linear growth with penetration depth and shows different slopes in different soil layers. This is because the outer frictional resistance is only related to the earth pressure acting on the pile and the interface property between soil and pile, so it is relatively stable.

On the other hand, the inner frictional resistance is influenced by the soil plugging-effect and soil-arching effect. It can be seen that the variation trend of the total frictional resistance is basically dominated by the inner frictional resistance. In Figures 11 and 12, the inner and total frictional resistance changed dramatically at 1.5 m, 3 m, and 4 m, which is related to the sudden change in the soil plug length in the previous section. When the soil plug length is stable, the soil-plugging effect is obvious, and the inner frictional resistance is large. On the other hand, when the soil plug length increases, evidently, denoting that the soil plug is in the formation or reformation stage, the soil plug and the pile slide during this kind of situation; the static friction changes into sliding friction, and the soil-arching effect fails, meaning the friction is low.

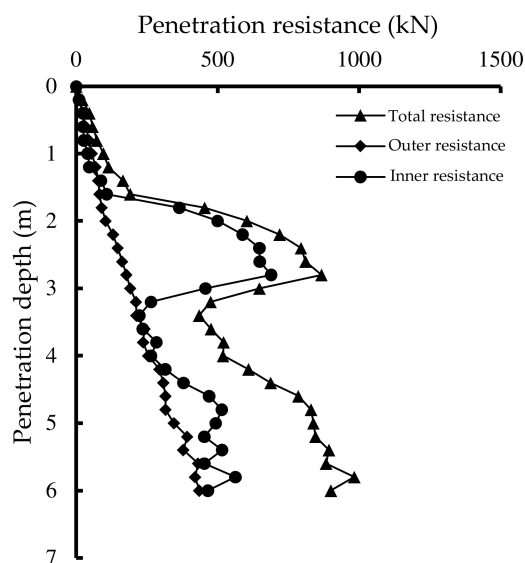


Figure 11. Penetration resistance curve for condition *a*.

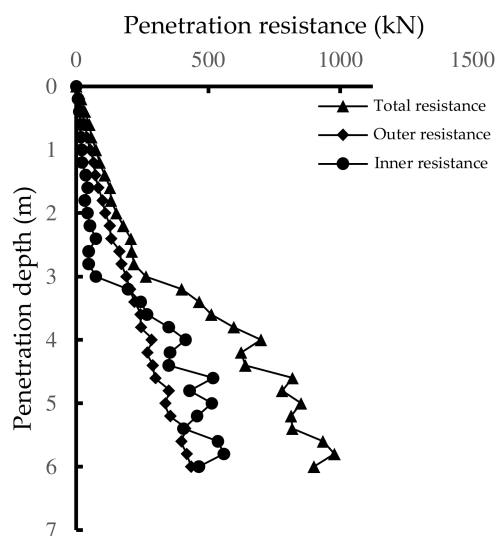


Figure 12. Penetration resistance curve for condition *b*.

5. Conclusions

By combining in situ test analysis and DEM simulation, this paper discusses the development mechanism of the soil-plugging effect on surface resistance during the penetration process of small-diameter jacked piles. Through the analysis of the test results and the comparison between the in-situ tests and the simulation results, it was found that the changing curve of pile penetration resistance of the two groups from the in situ tests showed a similar development pattern. Our detailed conclusion is as follows.

For the first test condition, penetration resistance increases with pile penetration depth, then decreases or remains unchanged after reaching a certain depth. Then, there is a second stage of continuous growth. For the second condition, the first stage was not observed. For both of the test conditions, the sudden change in pile penetration resistance occurred when the pile tip moved through the interface of two layers of soil, yet the depth of this sudden change was different for the two conditions.

The DEM analysis results show that the soil plug slides with the inner surface of the pile due to the difference in strength and stiffness between the different soil layers, which is the reason for the sudden change in the pile penetration resistance. When the soil layer is soft and hard, this phenomenon is relatively strong, which also explains the missing part of the first stage for condition *b*, as the first layer in the second condition is too soft for the soil plug to form quickly. The analysis results of this paper can be helpful for revealing the relationship between the soil-plugging effect of small-diameter jacked piles and the development of pile resistance and can also provide a reference for relevant engineering construction and design.

Future work includes the following aspects:

1. The influence of the simulation dimension of the DEM should be further discussed;
2. The friction characteristics between the soil and pile and the corresponding micromechanism should be studied;
3. A more accurate simulation method should be developed for the prediction of penetration resistance.

Author Contributions: X.W.: Data curation, Formal analysis, Writing—original draft. Writing—review & editing. Y.M.: Conceptualization, Funding acquisition, Methodology, Supervision. Y.Y.: Resources, Validation. R.W.: Visualization, Resources. D.Z.: Investigation, Writing—review & editing. All authors have read and agreed to the published version of the manuscript.

Funding: The research described in this paper was financially supported by the National Natural Science Foundation of China (Grant No. 52178302), the Key R & D Projects in Shaanxi Province (No. 2020SF-373, 2021SF-523), and the Natural Science Basic Research Program of Shaanxi [grant number 2022]Q-375].

Institutional Review Board Statement: Not applicable.

Informed Consent Statement: Not applicable.

Conflicts of Interest: The authors declare no conflict of interest.

References

1. Hoang, L.T.; Dao, K.X.; Xiong, X.; Matsumoto, T. Performance analysis of a jacked-in single pile and pile group in saturated clay ground. *Soils Found.* **2021**, *62*, 101094. [\[CrossRef\]](#)
2. Lehane, B.; Gavin, K. Base Resistance of Jacked Pipe Piles in Sand. *J. Geotech. Geoenvironmental Eng.* **2001**, *127*, 473–480. [\[CrossRef\]](#)
3. Vesić, A.S. Expansion of Cavities in Infinite Soil Mass. *J. Soil Mech. Found. Div.* **1972**, *98*, 265–290. [\[CrossRef\]](#)
4. Randolph, M.F.; Carter, J.P.; Wroth, C.P. Discussion: Driven piles in clay—The effects of installation and subsequent consolidation. *Géotechnique* **1981**, *31*, 291–295. [\[CrossRef\]](#)
5. Murthy, D.S.; Robinson, R.G.; Rajagopal, K. Formation of soil plug in open-ended pipe piles in sandy soils. *Int. J. Geotech. Eng.* **2021**, *15*, 519–529. [\[CrossRef\]](#)
6. Kou, H.-L.; Li, W.; Chu, J.; Yang, D.-L. Model tests on open-ended concrete pipe piles jacked in sand. *Mar. Georesources Geotechnol.* **2020**, *38*, 939–946. [\[CrossRef\]](#)
7. Li, J.; Li, L.; Sun, D.; Tang, J. Theoretical study on sinking resistance of jacked piles in saturated soft clay. *Chin. J. Geotech. Eng.* **2015**, *37*, 1454–1461.
8. Lehane, B.M.; Gill, D. Displacement fields induced by penetrometer installation in an artificial soil. *Int. J. Phys. Model. Geotech.* **2004**, *4*, 25–36. [\[CrossRef\]](#)
9. Cao, Z.; Kong, G.; Liu, H.; Zhou, H. Model tests on 3-D soil deformation during pile penetration using transparent soils. *Chin. J. Geotech. Eng.* **2014**, *36*, 395–400.
10. Liu, X.; Wang, Y.; Zhang, M. Application of Miniature FBG-MEMS Pressure Sensor in Penetration Process of Jacked Pile. *Micromachines* **2020**, *11*, 876. [\[CrossRef\]](#)
11. Sang, S.; Wang, Y.; Ma, J.; Zhang, M. Experimental Research Based on the Optical Fiber Sensing Technology for a Jacked PHC Pipe Pile Penetration Process. *Adv. Civ. Eng.* **2020**, *2020*, 8873308. [\[CrossRef\]](#)
12. Kodsý, A.; Iskander, M. Insights into Plugging of Pipe Piles Based on Pile Dimensions. *Appl. Sci.* **2022**, *12*, 2711. [\[CrossRef\]](#)
13. Kou, H.; Jing, H.; Zhou, N.; Chen, Q.; Li, W. Feasibility of bare fiber Bragg grating sensing technology in the measurement of inner wall axial stress along open-ended pipe pile in sand. *Struct. Control. Health Monit.* **2022**, *29*, e2920. [\[CrossRef\]](#)
14. Han, F.; Ganju, E.; Prezzi, M.; Salgado, R.; Zaheer, M. Axial resistance of open-ended pipe pile driven in gravelly sand. *Géotechnique* **2020**, *70*, 138–152. [\[CrossRef\]](#)
15. Engin, H.K.; Brinkgreve, R.B.J.; van Tol, A.F. Simplified numerical modelling of pile penetration—The press-replace technique. *Int. J. Numer. Anal. Methods Géoméch.* **2015**, *39*, 1713–1734. [\[CrossRef\]](#)
16. Henke, S. Influence of pile installation on adjacent structures. *Int. J. Numer. Anal. Methods Géoméch.* **2010**, *34*, 1191–1210. [\[CrossRef\]](#)
17. Daryaei, R.; Bakroon, M.; Aubram, D.; Rackwitz, F. Numerical evaluation of the soil behavior during pipe-pile installation using impact and vibratory driving in sand. *Soil Dyn. Earthq. Eng.* **2020**, *134*, 106177. [\[CrossRef\]](#)
18. Fan, S.; Bienen, B.; Randolph, M.F. Stability and efficiency studies in the numerical simulation of cone penetration in sand. *Géotechnique Lett.* **2018**, *8*, 13–18. [\[CrossRef\]](#)
19. Rooz, A.F.H.; Hamidi, A. A numerical model for continuous impact pile driving using ALE adaptive mesh method. *Soil Dyn. Earthq. Eng.* **2019**, *118*, 134–143. [\[CrossRef\]](#)
20. Tolooyan, A.; Gavin, K. Modelling the Cone Penetration Test in sand using Cavity Expansion and Arbitrary Lagrangian Eulerian Finite Element Methods. *Comput. Geotech.* **2011**, *38*, 482–490. [\[CrossRef\]](#)
21. Ko, J.; Jeong, S.; Lee, J.K. Large deformation FE analysis of driven steel pipe piles with soil plugging. *Comput. Geotech.* **2016**, *71*, 82–97. [\[CrossRef\]](#)
22. Galavi, V.; Beuth, L.; Coelho, B.Z.; Tehrani, F.S.; Hölscher, P.; Van Tol, F. Numerical Simulation of Pile Installation in Saturated Sand Using Material Point Method. *Procedia Eng.* **2017**, *175*, 72–79. [\[CrossRef\]](#)
23. Lorenzo, R.; da Cunha, R.; Neto, M.C.; Nairn, J. Numerical simulation of installation of jacked piles in sand using material point method. *Can. Geotech. J.* **2018**, *55*, 131–146. [\[CrossRef\]](#)
24. Phuong, N.; van Tol, A.; Elkadi, A.; Rohe, A. Numerical investigation of pile installation effects in sand using material point method. *Comput. Geotech.* **2016**, *73*, 58–71. [\[CrossRef\]](#)
25. Cyril, P.A.; Kok, S.T.; Song, M.K.; Chan, A.; Wong, J.-Y.; Choong, W.K. Smooth particle hydrodynamics for the analysis of stresses in soil around Jack-in Pile. *Eur. J. Environ. Civ. Eng.* **2022**, *26*, 94–120. [\[CrossRef\]](#)
26. Soleimani, M.; Weißenfels, C. Numerical simulation of pile installations in a hypoplastic framework using an SPH based method. *Comput. Geotech.* **2021**, *133*, 104006. [\[CrossRef\]](#)

27. Ciantia, M.O.; Arroyo, M.; Butlanska, J.; Gens, A. DEM modelling of cone penetration tests in a double-porosity crushable granular material. *Comput. Geotech.* **2016**, *73*, 109–127. [[CrossRef](#)]
28. Li, L.; Wu, W.; Liu, H.; Lehane, B. DEM analysis of the plugging effect of open-ended pile during the installation process. *Ocean Eng.* **2021**, *220*, 108375. [[CrossRef](#)]
29. Hong, J.; Xueyi, Y. Study on Computer Numerical Simulation of Driving Static Pressure Pile. *Phys. Procedia* **2012**, *24*, 686–691. [[CrossRef](#)]
30. Hu, W.; Le, Y.; Wang, N.; Liu, D.; Xu, C.; Min, J. Response of open-end pipe piles to vertical dynamic load considering the effects of soil plug and soil disturbance during driving. *Soil Dyn. Earthq. Eng.* **2019**, *125*, 105700. [[CrossRef](#)]
31. Liu, J.; Duan, N.; Cui, L.; Zhu, N. DEM investigation of installation responses of jacked open-ended piles. *Acta Geotech.* **2019**, *14*, 1805–1819. [[CrossRef](#)]
32. O'Sullivan, C. Particle-Based Discrete Element Modeling: Geomechanics Perspective. *Int. J. Géoméch.* **2011**, *11*, 449–464. [[CrossRef](#)]
33. Mei, Y.; Zhou, D.; Wang, X.; Zhao, L.; Shen, J.; Zhang, S.; Liu, Y. Deformation Law of the Diaphragm Wall during Deep Foundation Pit Construction on Lake and Sea Soft Soil in the Yangtze River Delta. *Adv. Civ. Eng.* **2021**, *2021*, 6682921. [[CrossRef](#)]
34. Wang, X.; Song, Q.; Gong, H. Research on Deformation Law of Deep Foundation Pit of Station in Core Region of Saturated Soft Loess Based on Monitoring. *Adv. Civ. Eng.* **2022**, *2022*, 7848152. [[CrossRef](#)]
35. Wang, X.Y.; Ma, Z.; Zhang, Y.T. Research on Safety Early Warning Standard of Large-Scale Underground Utility Tunnel in Ground Fissure Active Period. *Front. Earth Sci.* **2022**, *10*, 828477. [[CrossRef](#)]
36. Yuan, B.; Chen, W.; Zhao, J.; Yang, F.; Luo, Q.; Chen, T. The Effect of Organic and Inorganic Modifiers on the Physical Properties of Granite Residual Soil. *Adv. Mater. Sci. Eng.* **2022**, *2022*, 9542258. [[CrossRef](#)]
37. Su, D.; Wu, Z.; Lei, G.; Zhu, M. Numerical study on the installation effect of a jacked pile in sands on the pile vertical bearing capacities. *Comput. Geotech.* **2022**, *145*, 104690. [[CrossRef](#)]
38. Yuan, B.; Li, Z.; Chen, W.; Zhao, J.; Lv, J.; Song, J.; Cao, X. Influence of Groundwater Depth on Pile–Soil Mechanical Properties and Fractal Characteristics under Cyclic Loading. *Fractal Fract.* **2022**, *6*, 198. [[CrossRef](#)]
39. Yuan, B.; Chen, M.; Chen, W.; Luo, Q.; Li, H. Effect of Pile-Soil Relative Stiffness on Deformation Characteristics of the Laterally Loaded Pile. *Adv. Mater. Sci. Eng.* **2022**, *2022*, 4913887. [[CrossRef](#)]
40. Duan, N.; Cheng, Y.P.; Lu, M.; Wang, Z. Dem Investigation of Sand Response during Displacement Pile Installation. *Ocean. Eng.* **2021**, *230*, 109040. [[CrossRef](#)]
41. Jiang, M.; Dai, Y.; Cui, L.; Shen, Z.; Wang, X. Investigating mechanism of inclined CPT in granular ground using DEM. *Granul. Matter* **2014**, *16*, 785–796. [[CrossRef](#)]
42. Lobo-Guerrero, S.; Vallejo, L.E. Dem Analysis of Crushing Around Driven Piles in Granular Materials. *Géotechnique* **2005**, *55*, 617–623. [[CrossRef](#)]
43. Wang, J.; Zhao, B. Discrete-Continuum Analysis of Monotonic Pile Penetration in Crushable Sands. *Can. Geotech. J.* **2014**, *51*, 1095–1110. [[CrossRef](#)]
44. Zhu, N.; Cui, L.; Liu, J.; Wang, M.; Zhao, H.; Jia, N. Discrete Element Simulation On the Behavior of Open-Ended Pipe Pile Under Cyclic Lateral Loading. *Soil Dyn. Earthq. Eng.* **2021**, *144*, 106646. [[CrossRef](#)]